THE JOURNAL OF PHYSICAL CHEMISTRY A

Article

pubs.acs.org/JPCA

# How Short is the Strongest Hydrogen Bond in the Proton-Bound Homodimers of Pyridine Derivatives?

Andrey A. Gurinov,[†,‡] Stepan B. Lesnichin,[†] Hans-Heinrich Limbach,[†] and Ilya G. Shenderovich*[,†,‡,§]

[†]Institute of Chemistry and Biochemistry, Free University Berlin, Takustrasse 3, 14195 Berlin, Germany

[‡]St. Petersburg State University, 198504 St. Petersburg, Russian Federation

[§]Institute of Organic Chemistry, University of Regensburg, Universitaetstrasse 31, 93053 Regensburg, Germany

Supporting Information

**ABSTRACT:** Hydrogen bond geometries in the proton-bound homodimers of ortho-unsubstituted and ortho-methylsubstituted pyridine derivatives in aprotic polar solution were estimated using experimental NMR data. Within the series of homodimers studied the hydrogen bond lengths depend on the proton affinity of pyridines and—at least for the ortho-methylsubstituted pyridines—on the p$K_a$ of the conjugate acids in an approximately quadratic manner. The shortest possible hydrogen bond in the homodimers of ortho-unsubstituted pyridines is characterized by the N···N distance of 2.613 Å. Steric repulsion between the methyl groups of the ortho-methylsubstituted pyridines becomes operative at an N···N distance of ∼2.7 Å and limits the closest approach to 2.665 Å.

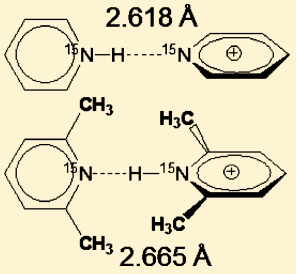


## INTRODUCTION

Hydrogen bonding (H-bonding) is a mandatory preliminary step to proton transport that is one of the main biochemical reactions.[1−5] Extensive studies of the last decades have allowed elucidation of a number of general trends. In the simplest case of an isolated complex of a proton donor A−H and a proton acceptor B in an aprotic solvent the H-bond geometry depends both on the medium and the partner molecules. The strength of the electric field generated by surrounding molecules governs the shift of the binding proton toward the acceptor. This effect can be followed experimentally.[6−8] The effect of the medium on H-bond geometries is minimized in the case of proton-bound homodimers of $[A\cdots H\cdots A]^-$ and $[B\cdots H\cdots B]^+$ types. In such complexes the proton affinities of the partners are the same, a circumstance that leads to the formation of strongly bound species. Two observations are remarkable. First, it is not guaranteed that the binding proton is located in the center of the H-bond if the proton affinities of the two partners are the same. Theoretical analyses for a broad range of bases have demonstrated that the primary factor that determines whether the $[B\cdots H\cdots B]^+$ H-bond is symmetric (the proton is equally shared) or asymmetric (the proton is located at one of the partners) is the electronegativity of B.[9,10] Thus, generally, H-bonds in proton-bound homodimers are symmetric for fluorine, oxygen, and sp-hybridized nitrogen bases, while asymmetric for $sp^2$- and $sp^3$-hybridized nitrogen bases.[9] Of course, the asymmetry can be induced or increased by steric hindrance. Second, within a series of closely related species, the binding energy of $[B\cdots H\cdots B]^+$ is correlated with the proton affinity in approximately quadratic manner.[11] This dependence is a result of the competition between the contribution in the binding energy that is lost due to the partial deprotonation of $[B-H]^+$ and the one that is gained by the partial protonation of B.[11] Thus, for each series of closely related species, there is one that forms the most stable proton-bound homodimer.

The objectives of the present work are to study experimentally (i) the correlation between the geometry of proton-bound homodimers and the proton-accepting ability of the molecules forming these complexes; (ii) the effect of steric hindrance on this correlation; (iii) the influence of the counterion on the structure of proton-bound homodimers. For these purposes, we have measured $^1$H NMR chemical shifts and $J_{^{15}N^1H}$ spin−spin scalar coupling in protonated bases and proton-bound homodimers for two series of ortho-unsubstituted and ortho-methylsubstituted pyridines in the slow intermolecular exchange regime. These parameters were used to estimate the H-bond geometry of the homodimers. The symmetry of these homodimers was proved by the sign of the primary isotope effect on the NMR chemical shift: $^p\Delta(H/D) \equiv \delta(\mathrm{N\underline{D}N}) - \delta(\mathrm{N\underline{H}N})$. Here, $\delta(\mathrm{N\underline{D}N})$ and $\delta(\mathrm{N\underline{H}N})$ stand for the deuteron and proton chemical shifts, respectively. The pyridines derivatives, the general view of their proton-bound homodimers, and the counteranions under study are shown in Figure 1a−h, Figure 1i, and Figure 1j,k, respectively.

## EXPERIMENTAL SECTION

**Materials.** Chemicals, if not otherwise stated, were purchased from Sigma-Aldrich and used without additional purification. The deuterated freon gas mixture $CDF_3/CDClF_2$ for the low-temperature NMR experiments, whose composition varied between 1:2 and 1:3, was prepared from chloroform-$d_1$

Received: August 13, 2014
Revised: October 16, 2014
Published: October 20, 2014

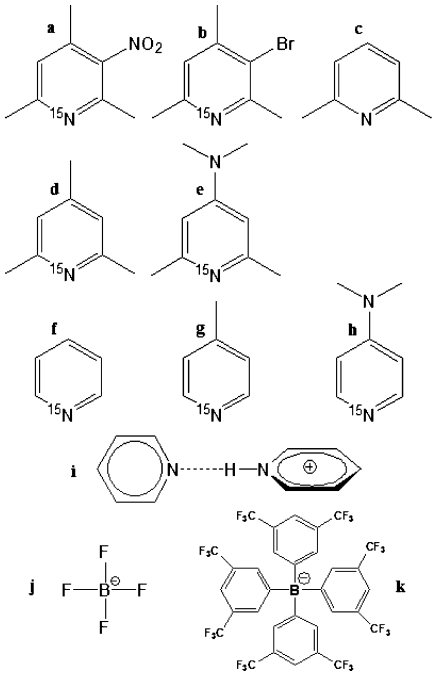

**Figure 1.** Pyridine derivatives (**a**–**h**), the general view of their proton-bound homodimers (**i**), and anions (**j**–**k**) used in this work. 2,4,6-Trimethyl-3-nitropyridine-$^{15}$N (**a**), 3-bromo-2,4,6-trimethylpyridine-$^{15}$N (**b**), 2,6-dimethylpyridine (**c**), 2,4,6-trimethylpyridine-$^{15}$N (**d**), *N*,*N*-2,6-tetramethylpyridin-4-amine-$^{15}$N (**e**), pyridine-$^{15}$N (**f**), 4-methylpyridine-$^{15}$N (**g**), *N*,*N*-dimethylpyridin-4-amine-$^{15}$N (**h**), tetrafluoroborate ($[BF_4]^-$) (**j**), and tetrakis[3,5-bis(trifluoromethyl)-phenyl]borate ($[BArF]^-$) (**k**).

as described recently.[7] The dielectric constant of this mixture at 120 K is ∼30.[7]

$^{15}$N-Enriched 2,4,6-trimethylpyridine, $^{15}$N-enriched pyridine, and $^{15}$N-enriched *N*,*N*-dimethylpyridin-4-amine were synthesized according to modified procedures based on refs 12, 13, and 14, respectively. The synthesis procedures of these compounds and of $^{15}$N-enriched 2,4,6-trimethyl-3-nitropyridine, $^{15}$N-enriched 3-bromo-2,4,6-trimethylpyridine, $^{15}$N-enriched *N*,*N*-2,6-tetramethylpyridin-4-amine, and $^{15}$N-enriched 4-methylpyridine are described in detail in the Supporting Information. 2-Ethoxy-4-methyl-3,4-dihydro-2*H*-pyran was synthesized according to procedure reported in ref 15. 4-Dimethylamino-2,6-dimethylpyrylium iodide was synthesized as described in refs 16 and 17. $^{15}$N-Enriched *N*-4-(pyridyl)-pyridinium chloride was synthesized according to procedure based on ref 14. Sodium tetrakis[3,5-bis(trifluoromethyl)-phenyl]-borate (BArF-Na) was prepared as described recently.[18]

**Complexes.** The general procedure of preparing complexes of bases with tetrafluoroboric acid was as follows. The equimolar quantities of the base and $HBF_4$ (50% aqueous solution) were mixed in dichloromethane and stirred for 3 h at 30 °C. Dichloromethane and water were then removed by repeated azeotropic distillation leaving a solid product.

The general procedure of obtaining complexes of protonated bases with $[BArF]^-$ was as follows. Equimolar amounts of the base and BArF-Na were mixed in 10 mL of water with a drop of 37% HCl and stirred for 12 h at 50 °C. The precipitated salt was filtrated, washed with water, and dried under vacuum.

The general procedure of obtaining proton-bound homodimers was as follows. Equimolar amounts of the base and the complex of the protonated base with $[BF_4]^-$ or $[BArF]^-$ were mixed directly in NMR tube.

Deuteration of complexes was performed by repeatedly dissolving them in methanol-OD (Eurisotop) and removing the solvent under vacuum.

**NMR Measurements.** Liquid-state $^1$H and $^{15}$N NMR spectra were measured on a Bruker AMX 500 spectrometer operated at 11.7 T equipped with a probe-head enabled to perform experiments down to 100 K. The $^1$H spectra were indirectly referenced to tetramethylsilane (TMS) by setting the central component of the residual $CHClF_2$ triplet of the freon mixture to 7.18 ppm.[7] The $^{15}$N spectra of free bases were indirectly referenced to pyridine dissolved in $CDF_3/CDClF_2$ (0 ppm). Bulk pyridine resonates at 277.6 ppm with respect to external solid $^{15}NH_4Cl$ and at −63.6 ppm with respect to external liquid nitromethane if the following relation $\delta$-($CH_3{}^{15}NO_2$, liquid) = $\delta(^{15}NH_4Cl$, solid) − 341.2 ppm[19,20] is taken into account. In contrast, the $^{15}$N chemical shifts of protonated bases and proton-bound homodimers were referenced directly to the corresponding free bases. The standard $^1$H and inverse-gated $^1$H-decoupled $^{15}$N NMR spectra were recorded with recycle times of 3 and 5 s, respectively.

The solid-state $^1$H NMR measurements were performed on a Bruker MSL−300 instrument operated at 7 T, equipped with a Varian 5 mm pencil CPMAS probe. The samples were spun under the magic-angle spinning (MAS) conditions. The spectra were indirectly referenced to bulk 3-(trimethylsilyl)propionic-2,2,3,3-$d_4$ acid sodium salt (0 ppm).

## RESULTS

In Figure 2 (p1−p3) are depicted NMR spectra of the proton-bound homodimer of pyridine-$^{15}$N in $CDF_3/CDF_2Cl$ obtained

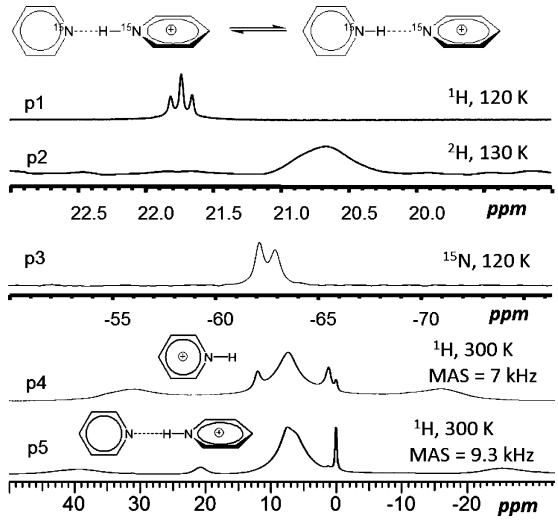


**Figure 2.** $^1$H (p1), $^2$H (p2), and $^{15}$N (p3) NMR spectra of the proton-bound homodimer of pyridine-$^{15}$N in $CDF_3/CDF_2Cl$ at 120/130 K. Solid-state $^1$H MAS NMR spectra of polycrystalline samples of the conjugate acid (p4) and the proton-bound homodimer (p5) of pyridine-$d_5$ at 300 K. Anion: $[BArF]^-$.

in the slow intermolecular exchange regime. These spectra are typical for the complexes under study and allow one to measure $^1$H, $^2$H, $^{15}$N NMR chemical shifts and $^1J_{^{15}N^1H}$ couplings with precision in the range of 0.01, 0.05, 0.1 ppm and 0.5 Hz, respectively. For the conjugate acid and the proton-bound homodimer of pyridine we also measured the values of the $^1$H


dx.doi.org/10.1021/jp5082033 | J. Phys. Chem. A 2014, 118, 10804−10812

NMR chemical shift of the mobile proton in the polycrystalline state, Figure 2 (p4 and p5). These values are 12.00 ± 0.05 and 20.73 ± 0.05 ppm, respectively. Pyridine-$d_5$ was used in the latter samples to minimize the line widths of the corresponding resonances.

The H-bond geometries of the conjugate acids and the proton-bound homodimers of pyridine derivatives depend on the counterion. This effect is demonstrated using $^1$H NMR spectra of the conjugate acids of the ortho-methylsubstituted derivatives **a** − **e** in Figure 3. For the conjugate acids the

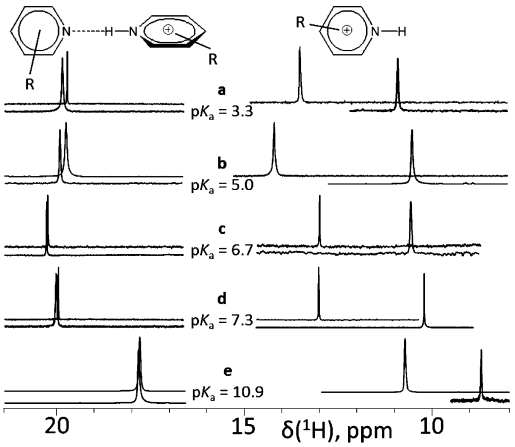


**Figure 3.** $^1$H NMR spectra of the conjugate acids (right) and the proton-bound homodimers (left) of ortho-methylsubstituted pyridine derivatives **a**−**e** in $CDF_3/CDF_2Cl$ at 120 K. Anions: $[BF_4]^-$ (upper spectra) and $[BArF]^-$ (lower spectra).

differences of the $^1$H NMR chemical shifts in complexes with $[BF_4]^-$ and $[BArF]^-$ are about 3 ppm, Table 1. For the proton-bound homodimers these differences are less than 0.1 ppm, Table 2. However, a strong interaction of the $[BF_4]^-$ anion with the proton-bound homodimers of ortho-unsubstituted pyridines favors intermolecular exchange that prevents the identification of NMR parameters of the mobile proton in these complexes even at 120 K. For the sake of simplicity, the spectra in Figure 3 have been obtained using nonlabeled pyridines.

**Table 1. Experimental NMR Parameters for the Pyridines and Their Conjugate Acids at 140 K**

| | | conjugate acid | | | |
|---|---|---|---|---|---|
| | | $[BF_4]^-$ | $[BArF]^-$ | | |
| base | $\delta(^{15}N)^a$ ± 0.1 ppm | $\delta(^1H)$ ± 0.01 ppm | $\delta(^1H)$ ± 0.01 ppm | $\lvert^1J_{^{15}N^1H}\rvert$ ± 0.5 Hz | $\Delta(^{15}N)^b$ ± 0.1 ppm |
| **a** | −2.2 | 13.54 | 10.79 | 94.6 | −119.5 |
| **b** | −3.3 | 14.19 | 10.49 | 93.8 | −118.7 |
| **c** | | 13.00 | 10.61 | | |
| **d** | −10.1 | 13.01 | 10.24 | 93.1 | |
| **e** | −35.8 | 10.73 | 8.69 | 94.6 | −114.6 |
| **f** | 0 | 14.2[c] | 10.8[c] | 96.0 | −123.0 |
| **g** | | 13.3[c] | 10.4[c] | 97.0 | −122.0 |
| **h** | | 11.6[c] | 8.9[c] | 98.0 | −121.0 |

[a]Referenced to pyridine dissolved in $CDF_3/CDClF_2$ (0 ppm). [b]Difference to the corresponding free base. [c]Remarkably depends on temperature.

**Table 2. Experimental NMR Parameters for the Proton-Bound Homodimers at 120 K**

| | $[BF_4]^-$ | | $[BArF]^-$ | | | |
|---|---|---|---|---|---|---|
| base | $\delta(^1H)$ ± 0.01 ppm | $\lvert^1J_{^{15}N^1H}\rvert$ ± 0.5 Hz | $\Delta(^{15}N)^a$ ± 0.1 ppm | $\lvert^1J_{^{15}N^1H}\rvert$ ± 0.5 Hz | $\delta(^1H)$ ± 0.01 ppm | $\Delta(H/D)^b$ ± 0.05 ppm |
| **a** | 19.69 | | −67.0 | 41.2 | 19.80 | |
| **b** | 19.76 | | −64.5 | 40.8 | 19.84 | −0.72 |
| **c** | 20.26 | | | | 20.24 | −0.79 |
| **d** | 19.92 | 40.7 | −60.4 | 40.4 | 20.0 | −0.76 |
| **e** | 17.73 | 42.0 | −50.9 | 42.0 | 17.76 | −0.39 |
| **f**[c] | | | −62.7 | 40.4 | 21.73 | −0.95[d] |
| **g** | | | −62[e] | 41.0 | 21.2[f] | |
| **h** | | | −57[e] | 40.5 | 18.9[f] | |

[a]Difference to the corresponding free base. [b]The primary isotope effect on the NMR chemical shift $^p\Delta(H/D) \equiv \delta(N\underline{D}N) - \delta(N\underline{H}N)$. [c]Reference 21. [d]At 130 K. [e] ± 1 ppm. [f] ± 0.1 ppm.

For the proton-bound homodimers of pyridine derivatives **b**−**e** deuteration of the H-bond results in strong, negative primary isotope effects on the NMR chemical shifts: $^p\Delta(H/D) \equiv \delta(N\underline{D}N) - \delta(N\underline{H}N)$, Figure 4. The spectra (b−d) and (e)

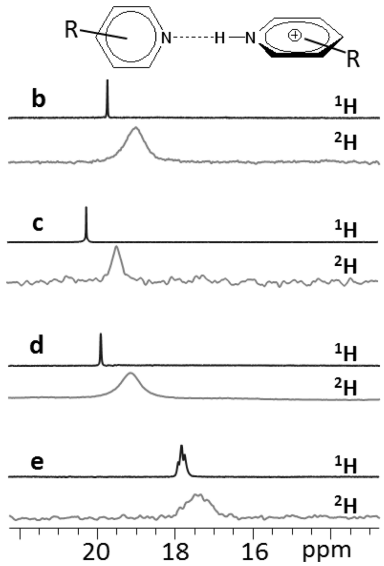


**Figure 4.** $^1$H (upper) and $^2$H (lower) NMR spectra of the proton-bound homodimers of ortho-methylsubstituted pyridine derivatives **b**−**e** in $CDF_3/CDF_2Cl$ at 120 K. Anion: $[BArF]^-$.

in Figure 4 were obtained using non- and $^{15}$N-labeled pyridines, respectively. The absolute value of the effect correlates with the value of the $^1$H chemical shift, Table 2, and Figure 4b−e.

In Figure 5 are depicted typical $^{15}N\{^1H\}$ NMR spectra of the conjugate acids and the proton-bound homodimers of pyridine derivatives. The spectra are referenced to the corresponding free bases. Protonation of pyridine results in ∼120 ppm shift of the $^{15}$N resonance, Table 1. The $^{15}$N chemical shift in the proton-bound homodimers seems to depend linearly on the p$K_a$ of the pyridine, Figure 5a,b,d,e.

## DISCUSSION

The main results of the experiments described above can be summarized as follows. The size of $[BF_4]^-$ anion is insufficient to prevent a specific interaction with the proton-bound homodimers of ortho-unsibstituted pyridines. In contrast,


dx.doi.org/10.1021/jp5082033 | J. Phys. Chem. A 2014, 118, 10804−10812

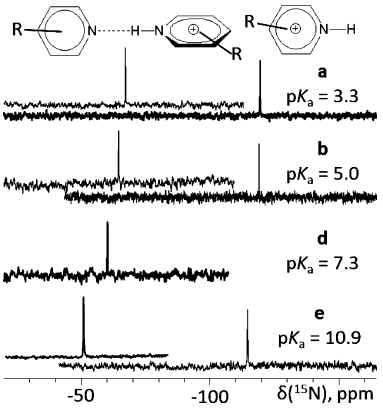


**Figure 5.** $^{15}$N{$^1$H} NMR spectra of the conjugate acids (lower) and the proton-bound homodimers (upper) of ortho-methylsubstituted pyridine derivatives **a**, **b**, **d**, and **e** in $CDF_3/CDF_2Cl$ at 120 K. Anion: $[BArF]^-$.

bulky, noncoordinating anion $[BArF]^-$ does affect neither geometry nor stability of H-bonds in associated cations. This conclusion agrees with other experimental data.[22] As a result, in the complexes with $[BArF]^-$ the values of $|^1J_{^{15}N^1H}|$ in the conjugate acids of both ortho-methylsubstituted and ortho-unsubstituted pyridines are close to the ones in the conjugate acids of ortho-*tert*-butylsubstituted pyridines.[23] The sign of the primary isotope effect on the NMR chemical shift clearly proves that the H-bonds in the proton-bound homodimers of pyridines are asymmetric.[24−26] The value of the effect is close to the highest known ones.[27,28] This finding, accompanied by the large values of the $^1$H NMR chemical shifts of the mobile protons, indicates that the H-bonds in question are very short. The multiplicity of the $^1$H NMR resonance indicates that the reversible proton transfer between the two pyridines is fast in the millisecond time scale down to 120 K. An IR study of proton-bound homodimers of pyridines in dichloromethane showed that proton transfer rates were slower than $10^{11}$ s$^{-1}$ up to 290 K.[29] The rate-limiting step for the proton transfer in the condensed phase is the solvent reorganization.[30−32] Note that in the gas phase the barrier for the proton transfer in these homodimers is expected to vary in a range of 4−20 kJ/mol.[29,33] Thus, the proton transfer rates in the gas phase are in a range of $10^{12}$ to $10^5$ s$^{-1}$.

To achieve the objectives of our work we need to attribute the obtained NMR parameters to H-bond geometry. Which of the obtained NMR parameters can be used to estimate H-bond geometries of the proton-bound homodimers of pyridines? Generally, $^{15}$N NMR chemical shifts represent the best possible parameter for the quantitative analyses of H-bond geometry in the case of pyridines.[34] The complexity of the system under study has no matter.[35−37] It is ironic that the proton-bound homodimers of pyridines represent a case where this parameter loses its advantage. Because of the reversible proton transfer, the experimentally observed $^{15}$N NMR chemical shift value is the mean of two others: one of the N−H bond and the other of the H···N bond. The latter values are not known. Since the lengths of the N−H and H···N bonds depend on each other one can "scan" over possible geometries for the mean $^{15}$N NMR chemical shift value that is the closest to the experimental one. However, the accuracy of such estimates will be low.[33] In contrast, geometry of H-bonds can be estimated on the basis of the experimental values of the $^1$H NMR chemical shift. The latter is not affected by the reversible proton transfer in the case of $[B{-}H{\cdots}B]^+$ species. The range of the primary isotope effect values on the chemical shift is sufficient for qualitative but not quantitative conclusions. Alternatively, the geometrical parameters of the proton-bound homodimers can be estimated from the experimentally observed $J_{^{15}N^1H}$ couplings. These couplings represent mean values: $\overline{J}_{^{15}N^1H} = (({}^1J_{^{15}N^1H} + {}^hJ_{^{15}N^1H})/2)$, where ${}^1J_{^{15}N^1H}$ and ${}^hJ_{^{15}N^1H}$ stand for the couplings across the N−H and H···N bonds, respectively. ${}^1J_{^{15}N^1H}$ is negative and depends on the N−H distance.[7,38,39] ${}^hJ_{^{15}N^1H}$ is negative for short H-bonds and changes its sign at the H···N distance of ∼1.62 Å.[40] The weaker is the H-bond, the closer is $\overline{J}_{^{15}N^1H}$ to $J_{^{15}N^1H}/2$. Thus, the H-bond geometries of the homodimers can be independently estimated using the experimental values of the $^1$H NMR chemical shift and the $\overline{J}_{^{15}N^1H}$ coupling.

**1. Experimental Estimation of H-Bond Geometry.** For a detailed discussion about geometric and NMR parameter correlations for H-bonds, refer to other publications.[41−44] Here, we introduce only the conceptual idea of these correlations.

According to the valence bond order concept, one can associate to any A−H···B hydrogen bond two valence bond orders given by $p_1 = \exp\{-(r_1 - r_1^0)/b_1\}$ and $p_2 = \exp\{-(r_2 - r_2^0)/b_2\}$, where $r_1$ and $r_2$ stand for A−H and H···B distances, $r_1^0$ and $r_2^0$ represent the equilibrium distances in the fictive diatomic units AH and HB, and $b_1$ and $b_2$ describe bond order decays with increasing bond distances. The total valence of hydrogen is unity; that is, $p_1 + p_2 = 1$. Thus, the distances $r_1$ and $r_2$ depend on each other. To incorporate this fact into the analysis one defines the natural hydrogen bond coordinates $q_1$ and $q_2$ according to $q_1 = (r_1 - r_2)/2$ and $q_2 = r_1 + r_2$. In the case of a linear H-bond these new coordinates have clear physical meanings: $q_1$ is the distance to the proton from the geometric center of the H-bond, and $q_2$ is the A···B distance. A detailed analysis of chemically and geometrically different H-bonds has demonstrated that it is not possible to describe both short and long H-bonds using the same parameters $r_1^0$, $r_2^0$, $b_1$, and $b_2$.[41] The problem can be solved by using empirical corrections for the bond orders. For the case of N−H···N hydrogen bonds these new bond orders are $p_1^* = p_1 - 250(p_1p_2)^5(p_1 - p_2) - 0.85(p_1p_2)^2$ and $p_2^* = p_2 - 250(p_1p_2)^5(p_2 - p_1) - 0.85(p_1p_2)^2$.[42] The numerical values of parameters are $r_1^0 = r_2^0 = 0.997$ Å, $b_1 = b_2 = 0.370$ Å.[42] Thus, we estimate the H-bond distances in the proton-bound homodimers as follows: $r_1 = -\ln(p_1^*)0.37$ Å + 0.997 Å, $r_2 = -\ln(p_2^*)0.37$ Å + 0.997 Å. Here and further we employ the empirically corrected bond orders instead of the conventional ones solely to reduce the number of parameters in use. This substitution can neither improve nor worsen remarkably the accuracy of our estimates.

The bond orders of the H-bonds in the proton-bound homodimers under study can be estimated from the experimental values of the $^1$H NMR chemical shift: $\delta(^1H) = \delta^0(^1H)(p_1^* + p_2^*) + \Delta_H 4p_1^*p_2^*$.[42,43] The parameter $\delta^0(^1H)$ stands for the limiting chemical shift in the fictive isolated conjugate acid of pyridine. In this work we take this parameter equal to the experimental value of $\delta(^1H)$ in the conjugate acid of the corresponding pyridine derivative with $[BArF]^-$, Table 1. $\Delta_H$ is an empirical fitting parameter. The value of this parameter is expected to be in the range of 10−20 ppm.[42,43,45] To reduce ambiguity in the choice of the value of this parameter we measured $^1$H NMR chemical shift in the proton-bound homodimer of pyridine in the polycrystalline state, $\delta(^1H) = 20.73$ ppm. The H-bond distances $r_1$ and $r_2$ in this complex are 1.123 and 1.532 Å. These values provide for $\Delta_H$ the value of 15.8 ppm. The H-bond distances in the other proton-bound


dx.doi.org/10.1021/jp5082033 | J. Phys. Chem. A 2014, 118, 10804−10812

homodimers under study estimated using the latter value are collected in Table 3. Are the numerical values of these distances realistic? Yes, the estimates obtained for the proton-bound homodimer of pyridine suggest that the hydrogen bond becomes shorter in polar aprotic solvent as compared to the crystal. What is the margin of error for these estimates? It depends at least on the margin of error for $\delta(^1H)$. The latter is 0.01 ppm, which implies a very small distance error of ~0.0005 Å. However, the above-mentioned choice of the limiting chemical shift parameters $\delta^0(^1H)$ and $\Delta_H$ may lead to systematic errors that are larger but difficult to evaluate. On the other hand, the estimated distances will reproduce correctly changes of average H-bond geometries within a series of H-bonded systems of similar structure.

**Table 3. Geometry of H-Bonds in the Proton-Bound Homodimers Estimated from $\delta(^1H)$ and $\overline{J}^{15}_{N^1H}$**

| base | $pK_a$[a] | PA[b] kJ/mol | $r_{NH}$ Å | $r_{NN}$ Å |
|---|---|---|---|---|
| **a** | 3.3 | 930 | 1.100[c] 1.100[d] | 2.695[c] 2.697[d] |
| **b** | 5.0 | 970 | 1.108[c] 1.104[d] | 2.681[c] 2.688[d] |
| **c** | 6.7 | 970 | 1.115[c] | 2.670[c] |
| **d** | 7.3 | 990 | 1.118[c] 1.109[d] | 2.665[c] 2.680[d] |
| **e** | 10.9 | 1030 | 1.100[c] 1.091[d] | 2.697[c] 2.714[d] |
| **f** | 5.2 | 930 | 1.163[c] 1.109[d] | 2.618[c] 2.680[d] |
| **g** | 5.9 | 950 | 1.155[c] 1.102[d] | 2.624[c] 2.692[d] |
| **h** | 9.5 | 1010 | 1.123[c] 1.107[d] | 2.659[c] 2.682[d] |

[a]Reference 46. [b]Estimated at the B3LYP/6-311++G(d,p) level. [c]Estimated from $\delta(^1H)$. [d]Estimated from $|\overline{J}^{15}_{N^1H}|$. See text for details.

The same bond orders can be independently estimated from the experimental values of $\overline{J}^{15}_{N^1H}$: $|^1J^{15}_{N^1H}| = |^1J^{0\,15}_{N^1H}|p_1^* - 8\Delta J p_1^*(p_2^*)^2$.[39,45,47] The parameter $^1J^{0\,15}_{N^1H}$ stands for the limiting value in the fictive isolated conjugate acid. $\Delta J$ is an empirical fitting parameter. Formally, $^1J^{0\,15}_{N^1H}$ should be equal to the experimental value in the conjugate acid of the corresponding pyridine derivative with $[BArF]^-$, Table 1. However, a better simulation of experimental data was achieved when this parameter was taken equal to 115 Hz.[45] The value of $\Delta J$ should be ~20 Hz but has to be fitted to each type of complex.[39,45,47] To secure that our estimates of H-bond geometry on the base of $\delta(^1H)$ and $\overline{J}^{15}_{N^1H}$ are totally independent of each other, we have fitted $\Delta J$ in a way that $^1J^{15}_{N^1H}$ changes its sign at the N···H distance of 1.62 Å.[40] This restriction provides for $\Delta J$ a value of 24 Hz. Thus, $|\overline{J}^{15}_{N^1H}| = ((|^1J^{0\,15}_{N^1H}| - 8\Delta J p_1^* p_2^*)(p_1^* + p_2^*))/2$, where $|^1J^{0\,15}_{N^1H}| = 115$ Hz and $\Delta J = 24$ Hz. The H-bond distances in the proton-bound homodimers under study estimated using this equation are collected in Table 3. Do the numerical values of these distances agree with the values estimated on the base of $\delta(^1H)$? Yes, and the longer the H-bond is, the closer the values are. What is the margin of error for the new estimates? It depends at least on the margin of error for $\overline{J}^{15}_{N^1H}$. The latter is 0.5 Hz, which provides for the former margin of error a value of 0.005 Å. Again, the systematic error of these estimations cannot be evaluated at the current stage. The observed discrepancy between the two estimates is outside the margin of error. We attribute this discrepancy to the fact that the latter correlation has been initially established and tested for relatively short N···H distances. The problem cannot be solved just by changing the parameters $^1J^{0\,15}_{N^1H}$ and $\Delta J$. We also do not have enough data about the behavior of $^1J^{15}_{N^1H}$ at long N···H distances to improve the available correlation. For this reason we regard the estimates obtained on the base of $\overline{J}^{15}_{N^1H}$ as proof for the estimates obtained on the base of $\delta(^1H)$. However, we will use the latter ones in the following discussion.

**2. Geometry of Homodimer Versus the Proton-Accepting Ability of Pyridine.** Neither $pK_a$ nor the gas-phase proton affinity (PA) are physically justified parameters for the description of H-bond in aprotic polar solvent. However, these parameters are easily available and useful for a semiquantitative analysis. In Table 3 are collected the $pK_a$ values of the conjugate acids of the pyridine derivatives under study. The PA values were calculated as follows: PA = $\Delta H^{298}(B) + 5RT/2 - \Delta H^{298}(BH^+)$. Here $\Delta H^{298}(B)$ and $\Delta H^{298}(BH^+)$ stand for the sums of electronic and thermal enthalpies of a pyridine derivative and its conjugate acid at 298 K. The enthalpies were estimated at the B3LYP/6-311++G(d,p) level using the Gaussian 09.C.01 program package.[48] This level is sufficient to obtain correct values.[49,50] There is near-linear correlation between the PA and $pK_a$ values within the ortho-unsubstituted and ortho-methylsubstituted derivatives of pyridine, Figure 6. The only exception is **b**. A value obtained at the B3LYP/cc-pVTZ level is very close to the previous one. The use of the SDD pseudopotential with the keyword MWB28 for Br gives for **b** a PA value of 963 kJ/mol. We are not aware of any other estimation of the PA of this pyridine. Thus, the PA value of **b** is in doubt.

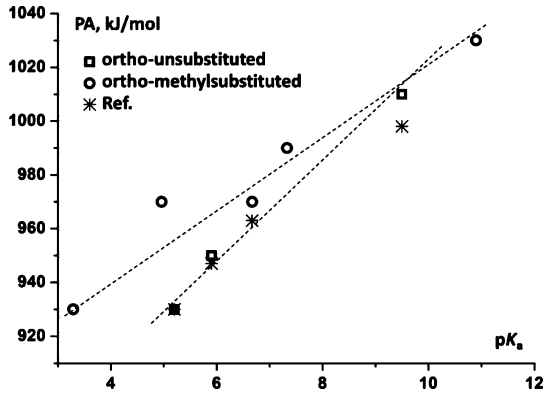


**Figure 6.** Gas-phase proton affinities (PA) of **f**–**h** (ortho-unsubstituted) and **a**–**e** (ortho-methylsubstituted) calculated at the B3LYP/6-311++G(d,p) level and adapted from ref 50 vs the $pK_a$ of conjugate acids.

In Figure 7 is depicted the N···N distance in the proton-bound homodimers of pyridines as a function of the $pK_a$ of conjugate acids and the PA of the pyridines. For the ortho-methylsubstituted pyridines these functions are $q_2 = 2.77 - (2.8 \times 10^{-2}) \times pK_a + (1.9 \times 10^{-3}) \times (pK_a)^2$ ($q_2$ in Å) and $q_2 = 14.06 - (2.327 \times 10^{-2}) \times PA + (1.188 \times 10^{-5}) \times PA^2$ ($q_2$ in Å, PA in kJ/mol). For the latter correlation we did not take into account the experimental data for **b**. Both correlations exhibit a minimum that corresponds to the shortest hydrogen bond achievable in the proton-bound homodimers of ortho-methylsubstituted pyridines.

For the ortho-unsubstituted pyridines these functions are $q_2 = 2.58 + (6 \times 10^{-3}) \times pK_a + (3 \times 10^{-4}) \times (pK_a)^2$ ($q_2$ in Å) and $q_2 = 5.47 - (6.36 \times 10^{-3}) \times PA + (3.54 \times 10^{-6}) \times PA^2$ ($q_2$ in Å, PA in kJ/mol). The former correlation fails to find a value of the $pK_a$ that would correspond to the shortest hydrogen bond achievable in the proton-bound homodimers of ortho-unsubstituted pyridines. In contrast, the latter correlation


dx.doi.org/10.1021/jp5082033 | J. Phys. Chem. A 2014, 118, 10804–10812

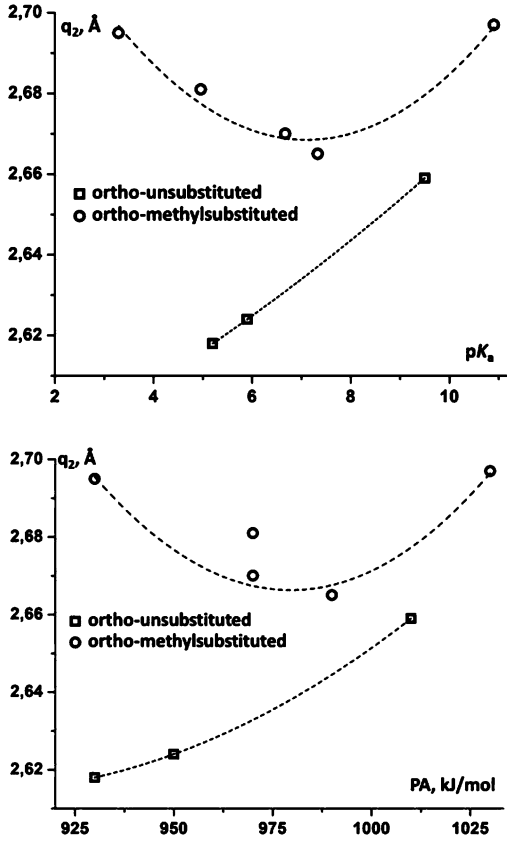


**Figure 7.** N···N distance ($q_2$) in the proton-bound homodimers of pyridines vs the p$K_a$ of conjugate acids (upper) and the gas-phase proton affinity (PA) of the pyridines (lower).

predicts that the shortest N···N distance of 2.613 Å will be realized in the proton-bound homodimers of an ortho-unsubstituted pyridine with PA of 900 kJ/mol. Note that calculations predict that the proton-bound homodimers of amines will show a maximum of the binding energy of 115 kJ/mol at PA of 900 kJ/mol.[9,11]

We conclude with a few related remarks. The H-bond in the proton-bound homodimer of **f** in the aprotic polar $CDF_3$/$CDClF_2$ mixture is shorter as compared to the crystalline state.[21] Thus, the indirect spin−spin coupling between the two $^{15}N$ nuclei of this homodimer, which cannot be measured in our experiments, should be larger than 10 Hz.[51] The interaction between the methyl groups of the two interacting molecules begins to dominate over the H-bond at the N···N distance of ∼2.7 Å. Indeed, at longer distances the functions $q_2$(PA) for the proton-bound homodimers of the ortho-methyl substituted and ortho-unsubstituted pyridines approach each other asymptotically, Figure 7. Note that ortho-*tert*-butyl substituted pyridines do not form proton-bound homodimers at all.[23]

**3. Geometrical and Spectral Features of Short NHN Hydrogen Bonds.** The present study states that the shortest NHN H-bonds in the proton-bound homodimers of pyridine derivatives exhibit N···N distances above 2.6 Å. These NHN H-bonds are longer than the shortest NHO and OHO hydrogen bonds. The limiting values for the N···O and O···O distances are ∼2.5 Å[52] and 2.4 Å,[53] respectively. However, the donor−acceptor distance is a useful measure of the strength of H-bonding only within a series of hydrogen bonds exhibiting a similar electronic structure. The following spectral features support this statement. The fundamental asymmetric stretching vibrations of the shared protons in the proton-bound homodimers of **f** and **d** are very broad bands with the first spectral moments at 2160 and 2250 $cm^{-1}$, respectively.[29] This feature is characteristic,[54] but prevents the use of this vibration as a measure of the H-bond geometry and energy. More useful for this purpose can be the out-of-plane bend $\gamma$(NH) that is located in the proton-bound homodimer of **f** at 822 $cm^{-1}$.[21] However, we are not aware of a correlation between the frequency of this vibration and H-bond parameters. Let us consider NHN H-bonds between $sp^3$-hybridized nitrogen bases. The most studied systems of this type are proton sponges.[54] The fundamental asymmetric stretching vibrations of the shared protons in proton sponges is ∼500 $cm^{-1}$. The limiting value for the N···N distance is ∼2.53 Å.[54] However, we can argue that these bonds are constrained by steric effects and are not necessarily linear. Thus, the length of such H-bonds should be calculated as a sum of the N−H and H···N distances. The proton-bound homodimers of ammonia and amines are better examples. In the former dimer the asymmetric stretching vibrations of the shared protons is shifted to 374 $cm^{-1}$, while the N···N distance is above 2.65 Å.[55,56] This geometry is close to a value of 2.636 Å in the proton-bound homodimer of trimethylamine.[57] A similar trend was observed in protonated tertiary diamines.[58] We conclude that H-bonds in the proton-bound homodimers of $sp^3$-hybridized nitrogen bases are stronger but not necessarily shorter as compared to the ones in the proton-bound homodimers of pyridine derivatives.

The kinetics of proton transfer in asymmetric proton-bound homodimers is related to the current discussion about the effect of steric strain and compression on the efficiency of enzyme-catalyzed reactions.[59−61] The rate constants of this transfer should depend on solvent and temperature. The quantization of the nuclear motion of the shared proton is an attractive task. It requires an explicit account for solvent molecules that is possible in multiscale hybrid quantum mechanics/molecular mechanics (QM/MM) molecular dynamics simulations.

## ■ CONCLUSION

In this work we have experimentally studied how the geometry of the proton-bound homodimers of pyridines depends on the p$K_a$ and the gas-phase proton affinity (PA) of the molecules forming these complexes. It is possible to reach the following conclusions from this study.

(i) The difference between the $^1H$ NMR chemical shift values of the mobile proton in the conjugate acids of ortho-unsubstituted and ortho-methylsubstituted pyridines with $[BArF]^-$ and $[BF_4]^-$ anion proves that the latter anion affects H-bond geometry in conjugated cations.

(ii) The negative values of the primary isotope effects on the NMR chemical shifts, $^p\Delta(H/D) \equiv \delta(N\underline{D}N) - \delta(N\underline{H}N)$, indicate that the H-bonds in the proton-bound homodimers of pyridines are asymmetric. This fact should be attributed to a low electronegativity of $sp^2$-hybridized nitrogen bases.[9] At the same time, these H-bonds are very short. As a result, in the aprotic polar $CDF_3/CDClF_2$ mixture the reversible proton transfer within these $[N{-}H{\cdots}N]^+$ H-bonds is fast in the millisecond time scale down to 120 K.

(iii) The shortest possible H-bond in the proton-bound homodimers of ortho-unsubstituted pyridines should be


dx.doi.org/10.1021/jp5082033 | J. Phys. Chem. A 2014, 118, 10804−10812

characterized by a N···N distance of 2.613 Å. Such complex will be formed by pyridines exhibiting a PA of 900 kJ/mol. Among the molecules studied, the proton-bound homodimer of pyridine shows the strongest H-bond with the N−H and N···N distances of 1.163 and 2.618 Å, respectively. Within the series of the proton-bound homodimers of ortho-unsubstituted pyridines the H-bond length correlates with the PA in approximately quadratic manner. In contrast, our data do not provide for the same series a reliable correlation between the H-bond geometry and the p$K_a$ values smaller than 5.2.

(iv) The shortest possible H-bond in the proton-bound homodimers of ortho-methylsubstituted pyridines is formed by 2,4,6-trimethylpyridine. This bond is characterized by the N−H and N···N distances of 1.118 and 2.665 Å, respectively. The interaction between the methyl groups begins to dominate over the H-bond at the N···N distance of ∼2.7 Å. Within the series of proton-bound homodimers of ortho-methylsubstituted pyridines the H-bond length correlates with both the PA and the p$K_a$ in approximately quadratic manner.

## ■ ASSOCIATED CONTENT

### Supporting Information

The synthesis procedures of $^{15}$N-enriched 2,4,6-trimethyl-3-nitropyridine, $^{15}$N-enriched 3-bromo-2,4,6-trimethylpyridine, $^{15}$N-enriched 2,4,6-trimethylpyridine, $^{15}$N-enriched *N*,*N*-2,6-tetramethylpyridin-4-amine, $^{15}$N-enriched pyridine, $^{15}$N-enriched 4-methylpyridine, and $^{15}$N-enriched *N*,*N*-dimethylpyridin-4-amine. This material is available free of charge via the Internet at http://pubs.acs.org.

## ■ AUTHOR INFORMATION


### Corresponding Author

*E-mail: Ilya.Shenderovich@chemie.uni-r.de.


### Notes

The authors declare no competing financial interest.

## ■ ACKNOWLEDGMENTS

This work was supported by the German-Russian Interdisciplinary Science Center (G-RISC) funded by the German Federal Foreign Office via the German Academic Exchange Service (DAAD) and the Russian Foundation for Basic Research (Project 14-03-00716). This work has benefited from discussions with Prof. G.S. Denisov, St. Petersburg State University. The authors gratefully acknowledge the Gauss Centre for Supercomputing e.V. (www.gauss-centre.eu) for funding this project by providing computing time on the GCS Supercomputer SuperMUC at Leibniz Supercomputing Centre (LRZ, www.lrz.de).

## ■ REFERENCES


(1) *Hydrogen-Transfer Reactions;* Hynes, J. T., Klinman, J. P., Limbach, H. H., Schowen, R. L., Eds.; Wiley-VCH: Weinheim, Germany, 2007; Vols. *1*−*4*.

(2) Borstnar, R.; Repic, M.; Kamerlin, S. C. L.; Vianello, R.; Mavri, J. Computational Study of the pK(a) Values of Potential Catalytic Residues in the Active Site of Monoamine Oxidase B. *J. Chem. Theory Comput.* **2012**, *8*, 3864−3870.

(3) Cleland, W. W.; Kreevoy, M. M. Low-Barrier Hydrogen-Bonds and Enzymatic Catalysis. *Science* **1994**, *264*, 1887−1890.

(4) Eigen, M. Proton transfer, acid-base catalysis, and enzymatic hydrolysis. I. Elementary processes. *Angew. Chem.* **1964**, *3*, 1−19.

(5) Baranov, M. S.; Lukyanov, K. A.; Borissova, A. O.; Shamir, J.; Kosenkov, D.; Slipchenko, L. V.; Tolbert, L. M.; Yampolsky, I. V.; Solntsev, K. M. Conformationally Locked Chromophores as Models of Excited-State Proton Transfer in Fluorescent Proteins. *J. Am. Chem. Soc.* **2012**, *134*, 6025−6032.

(6) Mauder, D.; Akcakayiran, D.; Lesnichin, S. B.; Findenegg, G. H.; Shenderovich, I. G. Acidity of Sulfonic and Phosphonic Acid - Functionalized SBA-15 under Almost Water - Free Conditions. *J. Phys. Chem. C* **2009**, *113*, 19185−19192.

(7) Shenderovich, I. G.; Burtsev, A. P.; Denisov, G. S.; Golubev, N. S.; Limbach, H.-H. Influence of the Temperature-Dependent Dielectric Constant on the H/D Isotope Effects on the NMR Chemical Shifts and the Hydrogen Bond Geometry of Collidine-HF Complex in CDF3/CDClF2 Solution. *Magn. Reson. Chem.* **2001**, *39*, S91−S99.

(8) Barnes, A. J.; Beech, T. R.; Mielke, Z. J. Strongly hydrogen-bonded molecular complexes studied by matrix-isolation vibrational spectroscopy. Part 1.—The ammonia−hydrogen chloride complex. *J. Chem. Soc., Faraday Trans.* **1984**, *80*, 455−463.

(9) Chan, B.; Del Bene, J. E.; Radom, L. What Factors Determine Whether a Proton-Bound Homodimer Has a Symmetric or an Asymmetric Hydrogen Bond? *Mol. Phys.* **2009**, *107*, 1095−1105.

(10) Reed, J. L. Electronegativity: Proton Affinity. *J. Phys. Chem.* **1994**, *98*, 10477−10483.

(11) Chan, B.; Del Bene, J. E.; Radom, L. Proton-Bound Homodimers: How Are the Binding Energies Related to Proton Affinities? *J. Am. Chem. Soc.* **2007**, *129*, 12197−12199.

(12) Golubev, N. S.; Smirnov, S. N.; Schah-Mohammedi, P.; Shenderovich, I. G.; Denisov, G. S.; Gindin, V. A.; Limbach, H.-H. Study of Acid-Base Interaction by Means of Low-Temperature NMR Spectra. Structure of Salicylic Acid. *Russ. J. Gen. Chem.* **1997**, *67*, 1082−1087.

(13) Whaley, T. W.; Ott, D. G. Syntheses with Stable Isotopes − Pyridine-N-15. *J. Labelled Compd.* **1974**, *10*, 283−286.

(14) Kumar, M.; Singh, S. K. Process for producing 4-(dimethylamino)pyridine by quaternization of pyridine and amination of pyridinium salt with DMF. US 2004106801 USA, 03 06 2004.

(15) Longley, R. I., Jr.; Emerson, W. S. The 1,4-Addition of Vinyl Ethers to α,β-Unsaturated Carbonyl Compounds. *J. Am. Chem. Soc.* **1950**, *72*, 3079−3081.

(16) King, L. C.; Ozog, F. J.; Moffat, J. Preparation of Substituted Mercaptopyrylium Salts. *J. Am. Chem. Soc.* **1951**, *73*, 300−302.

(17) King, L. C.; Ozog, F. J. Reactions of Pyrylium and Pyridinium Salts With Amines. *J. Org. Chem.* **1955**, *20*, 448−454.

(18) Yakelis, N. A.; Bergman, R. G. Safe Preparation and Purification of Sodium Tetrakis[(3,5-trifluoromethyl)phenyl]borate (NaBArF24): Reliable and Sensitive Analysis of Water in Solutions of Fluorinated Tetraarylborates. *Organometallics* **2005**, *24*, 3579−3581.

(19) Hayashi, S.; Hayamizu, K. Chemical-Shift Standards in High Resolution Solid-State NMR (2) N-15 Nuclei. *Bull. Chem. Soc. Jpn.* **1991**, *64*, 688−690.

(20) Witanowski, M.; Stefaniak, L.; Szymański, S.; Januszewski, H. External Neat Nitromethane Scale for Nitrogen Chemical-Shifts. *J. Magn. Reson.* **1977**, *28*, 217−226.

(21) Kong, S.; Borissova, A. O.; Lesnichin, S. B.; Hartl, M.; Daemen, L. L.; Eckert, J.; Antipin, M.Yu.; Shenderovich, I. G. Geometry and Spectral Properties of the Protonated Homodimer of Pyridine in the Liquid and Solid States. A Combined NMR, X-ray Diffraction and Inelastic Neutron Scattering Study. *J. Phys. Chem. A* **2011**, *115*, 8041−8048.

(22) Lesnichin, S. B.; Tolstoy, P. M.; Limbach, H.-H.; Shenderovich, I. G. Counteranion-Dependent Mechanisms of Intramolecular Proton Transfer in Aprotic Solution. *Phys. Chem. Chem. Phys.* **2010**, *12*, 10373−10379.

(23) Andreeva, D. V.; Ip, B.; Gurinov, A. A.; Tolstoy, P. M.; Denisov, G. S.; Shenderovich, I. G.; Limbach, H.-H. Geometrical Features of Hydrogen Bonded Complexes Involving Sterically Hindered Pyridines. *J. Phys. Chem. A* **2006**, *110*, 10872−10879.

(24) Schah-Mohammedi, P.; Shenderovich, I. G.; Detering, C.; Limbach, H.-H.; Tolstoy, P. M.; Smirnov, S. N.; Denisov, G. S.; Golubev, N. S. H/D-Isotope Effects on NMR Chemical Shifts and Symmetry of Homoconjugated Hydrogen-Bonded Ions in Polar Solution. *J. Am. Chem. Soc.* **2000**, *122*, 12878−12879.
(25) Gunnarsson, G.; Wennerström, H.; Egan, W.; Forsén, S. Proton and deuterium NMR of hydrogen bonds: Relationship between Isotope Effects and the Hydrogen Bond Potential. *Chem. Phys. Lett.* **1976**, *38*, 96−99.
(26) Altman, L. J.; Laugani, D.; Gunnarsson, G.; Wennerström, H.; Forsén, S. Proton, Deuterium, and Tritium Nuclear Magnetic Resonance of Intramolecular Hydrogen Bonds. Isotope Effects and the Shape of the Potential Energy Function. *J. Am. Chem. Soc.* **1978**, *100*, 8264−8266.
(27) Filarowski, A. Intramolecular Hydrogen Bonding in O-Hydroxyaryl Schiff Bases. *J. Phys. Org. Chem.* **2005**, *18*, 686−698.
(28) Vener, M. V. Model Study of the Primary H/D Isotope Effects on the NMR Chemical Shift in Strong Hydrogen-Bonded Systems. *Chem. Phys.* **1992**, *166*, 311−316.
(29) Melikova, S. M.; Rutkowski, K. S.; Gurinov, A. A.; Denisov, G. S.; Rospenk, M.; Shenderovich, I. G. FTIR study of the hydrogen bond symmetry in protonated homodimers of pyridine and collidine in solution. *J. Mol. Struct.* **2012**, *1018*, 39−44.
(30) Perrin, C. L. Symmetry of Hydrogen Bonds in Solution. *Pure Appl. Chem.* **2009**, *81*, 571−583.
(31) Perrin, C. L.; Karri, P. Are There Single-Well Hydrogen Bonds in Pyridine-Dichloroacetic Acid Complexes? *Chem. Commun.* **2010**, *46*, 481−483.
(32) Perrin, C. L.; Burke, K. D. Variable-Temperature Study of Hydrogen-Bond Symmetry in Cyclohexene-1,2-dicarboxylate Monoanion in Chloroform-d. *J. Am. Chem. Soc.* **2014**, *136*, 4355−4362.
(33) Shenderovich, I. G. Qualitative Analysis of the Geometry of the Hydrogen Bond in the Homoconjugated Pyridine Ion. *Russ. J. Gen. Chem.* **2007**, *77*, 620−625.
(34) Lorente, P.; Shenderovich, I. G.; Golubev, N. S.; Denisov, G. S.; Buntkowsky, G.; Limbach, H.-H. 1H/15N NMR Chemical Shielding, Dipolar 15N,2H Coupling and Hydrogen Bond Geometry Correlations in a Novel Serious of Hydrogen-Bonded Acid-Base Complexes of Collidine with Carboxylic Acids. *Magn. Reson. Chem.* **2001**, *39*, S18−S29.
(35) Lesnichin, S. B.; Shenderovich, I. G.; Muljati, T.; Limbach, H.-H.; Silverman, D. Intrinsic Proton Donating Power of Zinc-bound Water in a Carbonic Anhydrase Active Site Model Estimated by NMR. *J. Am. Chem. Soc.* **2011**, *133*, 11331−11338.
(36) Sharif, S.; Shenderovich, I. G.; González, L.; Denisov, G. S.; Silverman, D. N.; Limbach, H.-H. NMR and Ab initio Studies of Small Complexes Formed between Water and Pyridine Derivatives in Solid and Liquid Phase. *J. Phys. Chem. A* **2007**, *111*, 6084−6093.
(37) Shenderovich, I. G.; Buntkowsky, G.; Schreiber, A.; Gedat, E.; Sharif, S.; Albrecht, J.; Golubev, N. S.; Findenegg, G. H.; Limbach, H.-H. Pyridine-$^{15}$N - a Mobile NMR Sensor for Surface Acidity and Surface Defects of Mesoporous Silica. *J. Phys. Chem. B* **2003**, *107*, 11924−11939.
(38) Del Bene, J. E.; Alkorta, I.; Elguero, J. A Systematic Comparison of Second-Order Polarization Propagator Approximation and Equation-of-Motion Coupled Cluster Singles and Doubles C-C, C-N, N-N, C-H, and N-H Spin-Spin Coupling Constants. *J. Phys. Chem. A* **2009**, *113*, 12411−12420.
(39) Shenderovich, I. G.; Tolstoy, P. M.; Golubev, N. S.; Smirnov, S. N.; Denisov, G. S.; Limbach, H.-H. Low-Temperature NMR Studies of the Structure and Dynamics of a Novel Series of Acid-Base Complexes of HF with Collidine Exhibiting Scalar Couplings Across Hydrogen Bonds. *J. Am. Chem. Soc.* **2003**, *125*, 11710−11720.
(40) Del Bene, J. E.; Elguero, J. Systematic ab Initio Study of $^{15}$N−$^{15}$N and $^{15}$N−$^{1}$H Spin−Spin Coupling Constants Across N−H$^{+}$−N Hydrogen Bonds: Predicting N−N and N−H Coupling Constants and Relating Them to Hydrogen Bond Type. *J. Phys. Chem. A* **2006**, *110*, 7496−7502.
(41) Limbach, H.-H.; Tolstoy, P. M.; Pérez-Hernández, N.; Guo, J.; Shenderovich, I. G.; Denisov, G. S. OHO Hydrogen Bond Geometries and NMR Chemical Shifts: From Equilibrium Structures to Geometric H/D Isotope Effects, with Applications for Water, Protonated Water, and Compressed Ice. *Isr. J. Chem.* **2009**, *49*, 199−216.
(42) Pietrzak, M.; Shibl, M. F.; Broring, M.; Kuhn, O.; Limbach, H.-H. $^{1}$H/$^{2}$H NMR Studies of Geometric H/D Isotope Effects on the Coupled Hydrogen Bonds in Porphycene Derivatives. *J. Am. Chem. Soc.* **2007**, *129*, 296−304.
(43) Limbach, H.-H.; Pietrzak, M.; Sharif, S.; Tolstoy, P. M.; Shenderovich, I. G.; Smirnov, S. N.; Golubev, N. S.; Denisov, G. S. NMR-Parameters and Geometries of OHN- and ODN Hydrogen Bonds of Pyridine-Acid Complexes. *Chem.—Eur. J.* **2004**, *10*, 5195−5204.
(44) Ip, B. C. K.; Shenderovich, I. G.; Tolstoy, P. M.; Frydel, J.; Denisov, G. S.; Buntkowsky, G.; Limbach, H.-H. NMR Studies of Solid Pentachlorophenol-4-Methylpyridine Complexes Exhibiting Strong OHN Hydrogen Bonds: Geometric H/D Isotope Effects and Hydrogen Bond Coupling Cause Isotopic Polymorphism. *J. Phys. Chem. A* **2012**, *116*, 11370−11387.
(45) Tolstoy, P. M.; Smirnov, S. N.; Shenderovich, I. G.; Golubev, N. S.; Denisov, G. S.; Limbach, H.-H. NMR Studies of Solid State - Solvent and H/D Isotope Effects on Hydrogen Bond Geometries of 1:1 Complexes of Collidine with Carboxylic Acids. *J. Mol. Struct.* **2004**, *700*, 19−27.
(46) Calculated using Advanced Chemistry Development (ACD/Labs) Software V11.02 (© 1994−2014 ACD/Labs).
(47) Benedict, H.; Shenderovich, I. G.; Malkina, O. L.; Malkin, V. G.; Golubev, N. S.; Denisov, G. S.; Limbach, H.-H. Nuclear Scalar Spin-Spin Couplings and Geometries of Hydrogen Bonds. *J. Am. Chem. Soc.* **2000**, *122*, 1979−1988.
(48) Frisch, M. J.; Trucks, G. W.; Schlegel, H. B.; Scuseria, G. E.; Robb, M. A.; Cheeseman, J. R.; Scalmani, G.; Barone, V.; Mennucci, B.; Petersson, G. A.; et al. *Gaussian 09*, Revision C.1; Gaussian, Inc.: Wallingford, CT, 2009.
(49) Moser, A.; Range, K.; York, D. M. Accurate Proton Affinity and Gas-Phase Basicity Values for Molecules Important in Biocatalysis. *J. Phys. Chem. B* **2010**, *114*, 13911−13921.
(50) Hunter, E. P. L.; Lias, S. G. Evaluated Gas Phase Basicities and Proton Affinities of Molecules: an Update. *J. Phys. Chem. Ref. Data* **1998**, *27*, 413−656.
(51) Claramunt, R. M.; Perez-Torralba, M.; Maria, D. S.; Sanz, D.; Elena, B.; Alkorta, I.; Elguero, J. $^{15}$N-$^{15}$N Spin-Spin Coupling Constants Through Intermolecular Hydrogen Bonds in the Solid State. *J. Magn. Reson.* **2010**, *206*, 274−279.
(52) Steiner, T.; Majerz, I.; Wilson, C. C. First O−H−N Hydrogen Bond with a Centered Proton Obtained by Thermally Induced Proton Migration. *Angew. Chem., Int. Ed.* **2001**, *40*, 2651−2654.
(53) Steiner, T. The Hydrogen Bond in the Solid State. *Angew. Chem., Int. Ed.* **2002**, *41*, 48−76.
(54) Denisov, G. S.; Mavri, J.; Sobczyk, L. Potential Energy Shape for the Proton Motion in Hydrogen Bonds Reflected in Infrared and NMR Spectra. In: *Hydrogen Bonding—New Insights;* Grabowski, S., Ed.; Springer: Dordrecht, the Netherlands, 2006.
(55) Berthold, H. J.; Vonholdt, E.; Wartchow, R.; Vogt, T. X-ray and Neutron Diffraction Investigation at 298 K of NH4I···NH3 and ND4I···ND3 Containing the Cation H3N−H···NH3$^{+}$ and D3N−D···ND3$^{+}$. *Z. Kristallogr.* **1992**, *200*, 225−235.
(56) Yang, Y.; Kuehn, O. H/D Isotope Effects on the Geometry and Infrared Spectrum of the Protonated Ammonia Dimer. *Chem. Phys. Lett.* **2011**, *505*, 1−4.
(57) Bock, H.; Vaupel, T.; Schodel, H.; Koch, U.; Egert, E. Trialkylammonium-trialkylamine-tetraphenylborates [R3N$^{+}$-H···NR3] [B (C6H5)4] with Prototype N$^{+}$-H···N Hydrogen Bridges. *Tetrahedron Lett.* **1994**, *35*, 7355−7358.
(58) Beran, G. J. O.; Chronister, E. L.; Daemen, L. L.; Moehlig, A. R.; Mueller, L. J.; Oomens, J.; Rice, A.; Santiago-Dieppa, D. R.; Tham, F. S.; Theel, K.; Yaghmaeia, S.; Morton, T. H. Vibrations of a Chelated

Proton in a Protonated Tertiary Diamine. *Phys. Chem. Chem. Phys.* **2011**, *13*, 20380−20392.
(59) Hay, S.; Scrutton, N. S. Good Vibrations in Enzyme-Catalysed Reactions. *Nat. Chem.* **2012**, *4*, 161−168.
(60) Loveridge, E. J.; Behiry, E. M.; Guo, J.; Allemann, R. K. Evidence that a 'Dynamic Knockout' in Escherichia Coli Dihydrofolate Reductase Does Not Affect the Chemical Step of Catalysis. *Nat. Chem.* **2012**, *4*, 292−297.
(61) Kamerlin, S. C. L.; Mavri, J.; Warshel, A. Examining the Case for the Effect of Barrier Compression on Tunneling, Vibrationally Enhanced Catalysis, Catalytic Entropy and Related Issues. *FEBS Lett.* **2010**, *584*, 2759−2766.